Photocatalytic degradation of TCE in dry and wet air conditions with TiO_2 porous thin films

S. Suárez [a,*], N. Arconada [b], Y. Castro [b], J.M. Coronado [a,1], R. Portela [a], A. Durán [b], B. Sánchez [a]

[a] CIEMAT-PSA, Unidad de Aplicaciones Ambientales de la Radiación Solar, Avda. Complutense 22, 28040 Madrid, Spain
[b] Instituto de Cerámica y Vidrio (CSIC), Campus de Cantoblanco, 28049 Madrid, Spain

A B S T R A C T

Porous TiO_2-anatase thin films were prepared by the sol–gel route and used for the study of the influence of structural properties in their photocatalytic activity. Sols were prepared by using titanium isopropoxide with two types of modifier ligands, namely acetic acid and acetyl acetone, and pore generating agents such as polyethylene glycol, pluronic F-127 and polyethylene glycol hexadecyl ether (Brij 58). The photocatalytic activity for the degradation of trichloroethylene in air was evaluated under ultraviolet irradiation at different gas flows and water vapour contents. The photocatalytic activity depends on the nature of the pore generating agent which influences the TiO_2 crystallite size and the textural properties of the final material. The samples obtained by using acetic acid as the modifier ligand and either Brij 58 or PEG as the pore generating agent exhibited the best photocatalytic behaviour even in the presence of high quantities of water vapour. The direct trichloroethylene oxidation pathway to CO_2 is favoured at low water vapour contents, but an important generation of $COCl_2$ is observed even at low water partial pressures.

© 2011 Elsevier B.V. All rights reserved.

1. Introduction

Photocatalysis is a well known advanced oxidation process (AOP) for the abatement of volatile organic pollutants at mild conditions [1]. Trichloroethylene (TCE) is an organochloride compound that can be used as solvent, degreasing and/or cleaning agent [2,3]. TCE can be found in industrial emissions, landfills, hazardous waste disposal sites or indoor air. The interest in this molecule accounts to the presence of chlorine groups, which are involved in the photocatalytic process and the formation of several partial oxidation products. Thus, a relationship between changes in the physicochemical properties of the material and the CO_2 selectivity may be established. The excellence of TiO_2 as photocatalyst for the

removal of pollutants both in water and gas-phase is well known [4]. TiO_2 immobilisation is a requirement for the feasibility of the treatment of pollutants in air, mainly because it dodges the expensive filtration methods otherwise needed to avoid the release of nanoparticles into the atmosphere [5,6].

Sol–gel process is an effective, versatile and the most commonly used method to prepare immobilised TiO_2 thin films on glass support. Properties such as particle size and textural properties can be adjusted by varying the synthesis method [7]. To achieve a precise control on the final characteristics of the material, complexing agents such us β diketones (e.g. acetylacetone) or carboxylic acids (e.g. acetic acid) are frequently used [8–12].

Another approach to tailor the photocatalytic properties of semiconductors is to promote the formation of porous structures. The higher photocatalytic performance of TiO_2 porous films has been reported by several groups. Polyethylene glycol (PEG) is considered as the archetypal and most effective polymer template for the formation of macroporous TiO_2 thin films [13–18]. Surfactants

* Corresponding author. Tel.: +34 91 346 6177.
E-mail address: silvia.suarez@ciemat.es (S. Suárez).
[1] Current address: IMDEA-Energía, C/Tulipan S/n, Mostotes 28933 Madrid, Spain.

such as Triton [19] or Tween [20,21] have been used to synthesize nanocrystalline mesoporous TiO_2 films for the photodegradation of creatinine and methyl blue in water.

Phase composition, specific surface area, particle morphology, particle aggregation, bulk and surface OH groups and impurities are the most relevant parameters to describe the efficiency of photocatalysts [22,23]. However, the accurate comparison of samples synthesized by using different routes is complicated. Contradictory results can be found in the literature. While some authors claim the predominant role of the specific surface area [24,25] others point out to the crystalline degree as the main influence [26]. In previous work we have compared the photocatalytic performance of porous TiO_2 thin films prepared with PEG as the pore generating agent with that of dense films [27]. The final heat treatment temperature and time of sintering was optimized and the results show that the samples sintered at 450 °C for 1 h presented the best compromise between specific surface area and crystallinity resulting in a superior photocatalytic activity. Hitherto, no reports on the effect of the surfactant and nature of the chelating agent in the TCE conversion have been published.

Although the number of studies on the photo-oxidation of TCE is very high, the effect of water vapour partial pressure on the mineralization and formation of $COCl_2$ is elusive. Anderson et al. reported the conditions under which $COCl_2$ was not detected as reaction product [28,29]. Blake et al. showed the increase of the $COCl_2$ carbon atom product fraction with increasing the water vapour partial pressure [30]. Fan and Yates [31] indicated that the presence of water causes a decrease in the level of DCAC (dichloroacetylchloride) and $COCl_2$ enhancing the CO_2 yield. Amama et al. reported that humidification promotes the phosgene hydrolysis reaction [32].

In this article, the photocatalytic performance of TiO_2 thin films for the degradation of TCE is analysed. The role of different molecules such us polyethylene glycol, pluronic F-127 and polyethylene glycol hexadecyl ether (Brij 58) as pore generating agents and chelating agents such as acetylacetone or glacial acetic acid has been studied. To this end, experiments at different total flows and relative humidity content (R.H.) were performed.

2. Experimental

2.1. Synthesis of TiO_2 and photocatalysts preparation

Titania sols were prepared via acid catalysis by using titanium isopropoxide (TISP) as precursor. TISP was chemically modified by mixing it with acetylacetone (AcAc) or glacial acetic acid (AcOH). The molar ratio TISP/complexing agent was set to 1 in order to control hydrolysis and condensation reactions. The optimization of the synthesis parameters has been reported in a previous article [33]. The pore generating agents, provided by Sigma Aldrich, were incorporated to the sols in a surfactant/TISP molar ratio of 0.03 for polyethylene glycol (average molecular weight $400 \, g \, mol^{-1}$), 0.0005 for Pluronic F-127 (average molecular weight $12,600 \, g \, mol^{-1}$) and 0.07 for polyethylene glycol hexadecyl ether P5884 (Brij 58, average molecular weight $1124 \, g \, mol^{-1}$). Finally, a mix of ethanol and acidulated water (0.1 M HCl) was added drop by drop into the solutions. By following the same route two reference sols, one with AcAc and another with AcOH, were prepared without surfactant addition. Final molar ratio of 1 TISP:1 AcAc:40 EtOH:1 H_2O and TiO_2 concentration of $30 \, g \, L^{-1}$ were fixed. All the sols were maintained at room temperature before use.

Films were deposited by dip-coating onto glass-slides at a withdrawal rate of $25 \, cm \, min^{-1}$ for the reference sols and $35 \, cm \, min^{-1}$ for the sols containing pore generating agents. All coatings were treated at 450 °C for 1 h using a heating ramp of $10 \, °C \, min^{-1}$. Generally, all samples were prepared with two layers using an inter-medium heat treatment of 200 °C/30 min for dense coatings and 350 °C/1 h for porous coatings, after each coating deposition. In order to optimize the TiO_2 loading, AcOH-Brij-58 samples with one and three layers were prepared. For the evaluation of the photocatalytic activity the glass slides were coated with a first layer of SiO_2 [34] (200 nm) to avoid the diffusion of Na^+ cations from the glass substrate to the TiO_2 coating during firing.

2.2. Characterization of the coatings

Grazing X-ray diffraction (GXRD) studies were performed to analyse the crystallisation of TiO_2 in the anatase form and the crystal size, using $CuK\alpha$ radiation in a PANalytical's X'Pert PRO theta/theta diffractometer. The diffractograms were recorded in the range of 2θ 20–70°, using a fixed counting time of 20 s/step and an increment of 0.05°.

The hydrophobic/hydrophilic character of TiO_2 coatings deposited on silicon wafers was evaluated through the contact angle using an Easy Drop equipment ("Drop Shape Analysis System" Kruss DSA 100). Silicon wafers were selected as support in order to obtain values at similar conditions than the ones used to determine the pore size distribution by Environmental Ellipsometric Porosimetry (EEP) [35]. In this case, the EEP measurements were performed using the coating deposited on silicon wafer, in order to avoid the multiple reflections associated to the use of glass substrates that extend the overlapping and complicates the fit of the experimental data.

Ellipsometry and environmental ellipsometric porosimetry (EEP) measurements were performed using a spectral ellipsometer (WVASE32 ("Variable Angle Spectroscopic Ellipsometer") J.A. Co., Woollam M-2000UTM). This equipment is used for measuring optical constants and thicknesses of films simultaneously. The measured values are expressed as psi (ψ) and delta (Δ) and the fit of parameters in the range of wavelengths allows determining the thickness and the refractive index at the same time. Thickness (e) and refraction index (n) were measured evaluating their variations with the R.H. from 0 to 100% to calculate the adsorption–desorption isotherms. Pore size, pore volume, and specific surface area (S_s) of the films supported on silicon were determined from these isotherms following the approximation of Boissiere et al. [35]. An estimation of the exposed surface area per 1 cm^2 of sample was calculated considering the S_s, and thickness (cm). The density of the coatings was calculated using the Clausius Mossotti equation [36], and considering a refractive index of 2.4 for the bulk material.

2.3. Photocatalytic activity measurements

The photocatalytic oxidation of gas-phase trichloroethylene was studied in a continuous flow flat photoreactor with external dimensions $120 \, mm \times 50 \, mm \times 10 \, mm$ (length × width × depth). The photoreactor was made of stainless steel except for one face where a window of 30 cm^2, made out of borosilicate glass with low iron content, was placed for photocatalyst illumination, provided by two UVA (Philips TL-15 W/05) fluorescent lamps with a maximum emission at 365 nm wavelength. A gas mixture of TCE and air was fed from a gas cylinder of TCE/N_2 (Air Liquide, 500 ppm) and compressed air free of water and CO_2. Flow rate, pressure, temperature, UV radiation and R.H. were controlled by automated equipment using electronic mass flow controllers and automated valves. UV irradiation and water vapour content were measured using specific sensors, GaAsP photodiode for the former and a polymer sensing element in the latter. TCE concentration was fixed to 90 ppm, and the total gas flow varied between 200 and 400 $ml \, min^{-1}$ corresponding to gas hourly space velocities (GHSV) ranging between 5,000 and 10,000 h^{-1} (residence times between 0.74 s and 0.37 s). The study of the influence of

the R.H. (0–90%) on the photocatalytic activity was performed at 90 ppm TCE and 200 ml min^{-1} total flow. The gas composition was monitored continuously by using a FTIR Thermo-Nicolet 5700 spectrometer, equipped with a temperature controller multiple reflection gas cell (optical path 2 m) maintained a 110 °C. The gas cell and the optic of the system were continuously purged with pure air, eliminating thus the contribution of atmospheric carbon dioxide. Thus, the determination of the carbon dioxide concentration along the reaction time was evaluated. IR spectra of 64 scans at a resolution of 2 cm^{-1} were collected. The analysis of the reaction products was performed by following the evolution of the representative vibrational bands of the desired molecules at the following wavenumbers: TCE (965–903 cm^{-1}), CO_2 (2435–2233 cm^{-1}), $COCl_2$ (1873–1780 cm^{-1}), CO (2231–2027 cm^{-1}), HCl (2885–2662 cm^{-1}), DCAC-dichloroacetylchloride (1114–1037 cm^{-1}). The actual concentration of TCE, CO_2 and $COCl_2$ was evaluated against calibration mixtures provided by Air Liquide.

3. Results and discussion

3.1. Characterization of the TiO$_2$ films

The synthesis of the TiO$_2$ sols was optimized to obtain transparent and stable sols, since according to previous results, AcAc-sols displayed a yellowish colour [33]; meanwhile AcOH-sols were colourless. The synthesis of TiO$_2$ with F-127 and AcOH was ruled out because unstable sols were obtained in a wide range of compositions.

The crystallite size was estimated using Scherrer's equation from the GXRD peak broadening analysis (Table 1). In all cases, TiO$_2$-anatase was the only crystal phase observed (Fig. 1 supporting information). The addition of surfactants as pore generating agents inhibited the growth of crystallites and the aggregation of the primary particles as reported by Choi [37]. Thus, the reference material and TiO$_2$-AcAc-PEG presented similar values of crystalline domain size of 40 and 42 nm, while the coatings prepared from surfactant derived sols present a smaller crystalline domain size between 25 and 30 nm. FE-SEM analyses were performed to identify titania particle size (Fig. 2 supporting information). The calculation of the primary particle size by this technique is not a simple task. The micrographs indicate the presence of secondary particles with a Gaussian distribution of sizes and a mean size around 27 nm, in good agreement with XRD results. The size of titania primary particles ranges between 13 and 15 nm. Moreover, transmission electron microscopy (TEM) confirmed the presence of structures with porous in the range of the mesoporous. Bright and dark contrasts areas, corresponding to porous and titania matrix respectively, were identify for all samples (Fig. 3 supporting information).

The bands corresponding to C–H bonds vibrations (1550, 1450, 1350 and 1140 cm^{-1} [38,39]), C=C or C=O vibrations around 1650 and 1710 cm^{-1} and those at 2930 and 2870 cm^{-1}, associated to asymmetric and symmetric vibrations of CH$_2$ group, were not detected by FTIR spectroscopy, suggesting the elimination of most of the surfactants. Only a band at 435 cm^{-1} appears, assigned to the crystallisation of TiO$_2$ in the anatase phase [40] in agreement with GXRD results.

Spectral ellipsometry with water vapour technique allows determining the textural characteristics of mesoporous thin films. This is an extended and well known technique in the field of determination of the characteristics of mesoporous films [35,41–43]. Details concerning the characterization of sample by spectral ellipsometry can be found elsewhere [33].

This technique was used to study the structural characteristics of the porous coatings. Fig. 1 shows the adsorption–desorption

Table 1
Main characteristics of the TiO2-coating prepared with the different sols.

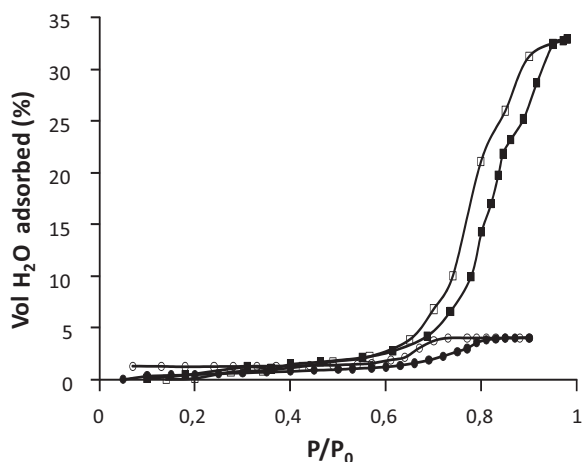| Composition	e (nm)	n (700 nm) ±0.05	Contact angle (°)	Density	Volume pore (%) ±5%	Pore size (nm) ±10%	S$_s$ (m²/cm³) ±10%	S$_s$ (m²/g) ±10%	Surface exposed per cm²/sample (cm²) ±10%	Crystal size ±10%
TiO$_2$-AcAc	170	2.11	50	3.66	–	–	–	–	–	40
TiO$_2$-AcOH	225	2.15	57	3.74	–	–	–	–	–	45
TiO$_2$-AcAc-PEG	180	2.09	32	3.63	4	10	8	2	0.7	42
TiO$_2$-AcAc-F127	200	1.75	53	2.78	28	10	55	20	7	25
TiO$_2$-AcAc-Brij58	250	1.77	38	2.80	27	11	43	15	5	33
TiO$_2$-	170 (1 layer)	1.70	32	2.64	32	11	74	28	13	29
AcOH-	250 (2 layers)	1.80	63	2.90	27	6	93	32	24	28
Brij58	360 (3 layers)	1.84	65	3.02	23	5	95	32	34	27

Fig. 1. Adsorption–desorption isotherms for TiO_2-AcAc-Brij58 (■ adsorption, □ desorption) and TiO_2-AcAc-PEG coatings (● adsorption, ○ desorption).

isotherms of TiO_2-AcAc-Brij 58 and TiO_2-AcAc-PEG obtained by EEP. The first coating presented a typical isotherm of a well-developed mesoporous material. A hysteresis loop between the adsorption and desorption branches was observed. The sharp drop on the desorption branch could be associated to mesoporous constrictions at the boundaries domains and/or smaller pores in the titania walls [44]. The pore size distribution from adsorption and desorption branches were 11 and 8 nm with a pore volume of 27% vol. For TiO_2 coating with PEG, the isotherm obtained is characteristic of a low porous material in the mesoporous range. In this case, pore size of 10 nm and pore volume of 4% was obtained.

Table 1 summarises the properties obtained by ellipsometric measurements (thickness, refraction index, pore volume, pore size, specific surface area and exposed surface) for all coatings. The incorporation of surfactants in the synthesis route leads to thicker layers and lower refractive indexes than the reference materials. For TiO_2-AcAc and TiO_2-AcAc-PEG coatings, the refractive index slightly changed from 2.11 to 2.09 suggesting that the coatings did not present porous in the mesoporous range. For the rest of compositions, lower refractive indexes were obtained and associated with higher pore volumes. The characteristic of porosity can be related to the properties of the surfactant. Thus, the porosity and the pore size increased with the hydrophobic tail length of the surfactant and with the surfactant concentration. In this case, the concentration was adjusted to obtain a similar pore size independently of the type of surfactant. Consequently similar high porosity (~30%) and pore size around 11 nm were obtained for TiO_2-AcAc-F-127 and TiO_2-AcOH/AcAc-Brij58 coatings.

In the case of TiO_2-AcOH-Brij58 multilayer coatings, the thickness and the refractive index increased with the number of coatings. The successive heat treatments after the incorporation of each layer provoked the partial collapse of the porosity. In this case, the pore size decreased from 11 to 5 nm while pore volume was reduced from 32 to 23%.

3.2. Photocatalytic results

The photocatalytic performance of TiO_2 thin films samples synthesised by using different pore generating agents and modifier ligands was evaluated in the TCE photo-oxidation reaction, using 90 ppm of TCE and residence times between 0.74 s and 0.37 s. Moreover the effect of film thickness and TiO_2 content was also evaluated. Finally experiments varying the R.H. of the gas stream were performed to analyse the partial oxidation products distribution in the presence of water vapour.
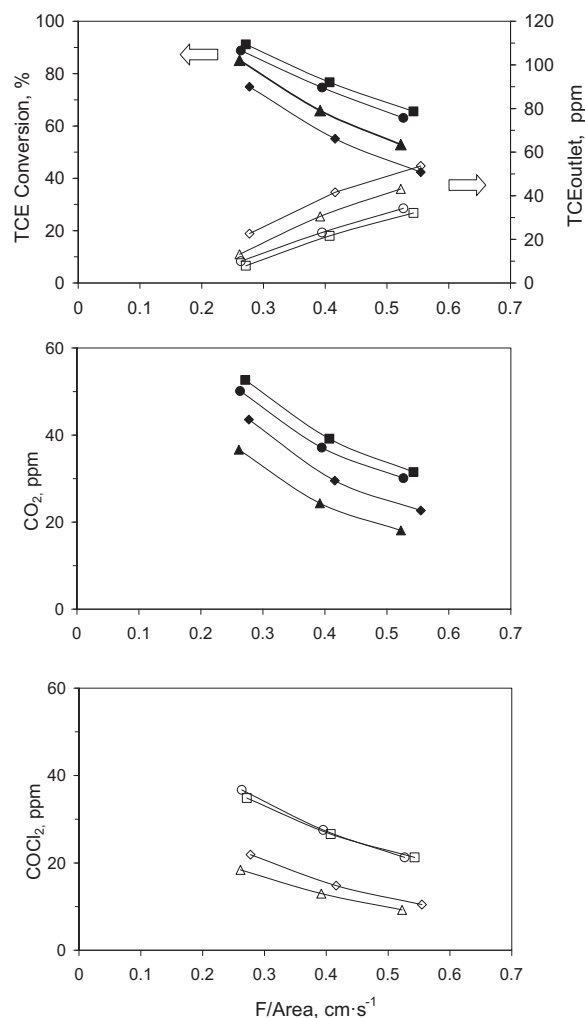

Fig. 2. Photocatalytic activity results obtained for dense and porous TiO_2 thin films prepared with acetylacetone and different pore generating agents: TiO_2- AcAc (♦, ◊), TiO_2-AcAc-Brij 58 (■, □), TiO_2-AcAc-PEG (●, ○), TiO2-AcAc-F127 (▲, △).

3.2.1. Influence of the synthesis route and TiO_2 loading

The photocatalytic oxidation of TCE at gas hourly space velocities between 5,000 and 10,000 h^{-1} for dense samples and for those prepared with PEG, F-127 and Brij 58 is represented in Fig. 2. TCE conversion and the formation of CO_2 and $COCl_2$ are shown in Fig. 2a–c, respectively, as a function of the ratio between total flow and illuminated sample area (F/A). As expected, TCE conversion decreased with the increasing total flow. The photocatalytic activity was clearly influenced by the incorporation of surfactants in the sol synthesis. The TCE conversion increased according to the following sequence: AcAc < AcAc-F-127 < AcAc-PEG ≤ AcAc-Brij-58. The TiO_2-AcAc coating showed significantly lower degradation of TCE likely associated to its dense structure. The incorporation of surfactants resulted in an important improvement of the photocatalytic activity mainly due to the porous structure of the films.

TiO_2-AcAc-Brij58 and TiO_2-PEG coatings reached conversions 30% and 27% higher than the TiO_2-AcAc reference material. Although the refractive index of TiO_2-PEG coating is high, it is suggested that PEG induces the appearance of an open porosity that sharply increases the hydrophilicity, as proved by the decrease of the contact angle. Such open porosity enhanced the adsorption capacity and thus, the photocatalytic activity. TiO_2-AcAc-Brij58 coating recorded the best efficiency in the series. The low contact angle of this catalyst suggests that its hydrophilic surface facilitates the adsorption of the contaminants hence improving its
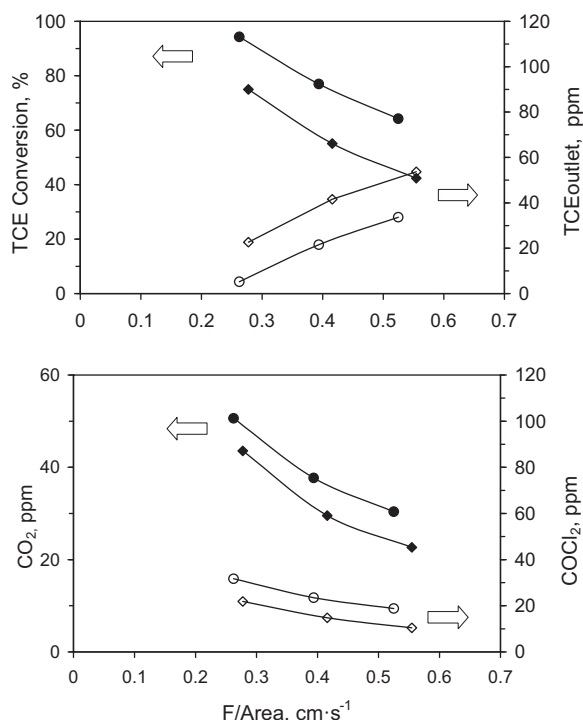
Fig. 3. Effect of the complexing agent on the TCE conversion and in the main reaction products for dense TiO_2 films: TiO_2-AcOH (●, ○), TiO_2-AcAc (♦, ◊).
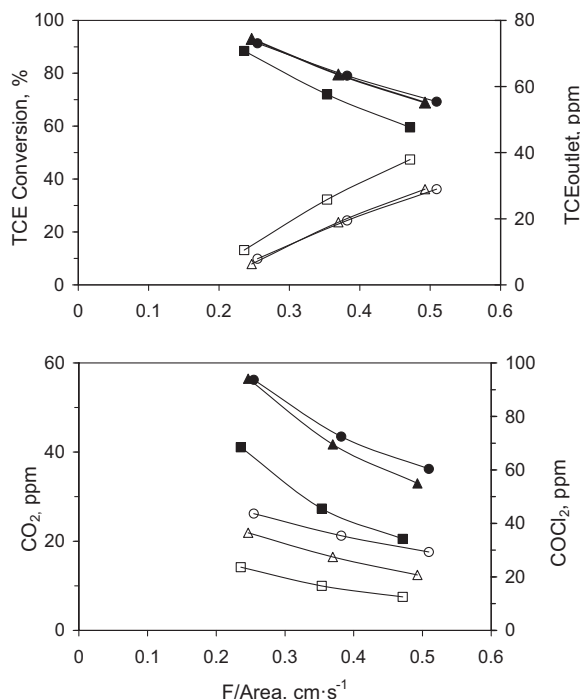

Fig. 4. Influence of TiO_2 thin film thickness in the photodegradation of TCE for TiO_2-AcOH-Brij 58 samples: 1 (■, □), 2 (▲, △), 3 (●, ○) layers.

photocatalytic activity [37,45]. During the heat treatment and elimination of the surfactant, the inorganic phase likely mimics the textural properties of the surfactant, modifying the hydrophilic/hydrophobic pore surfaces and, therefore, the photocatalytic performance of the coatings.

The main reaction products detected in the reaction outlet were CO_2 and $COCl_2$ (Fig. 2b and c). As previously reported, CO, DCAC (dichloroacetylchloride) and HCl were also detected in the outlet gas stream in minor amounts [46,47] (data not shown). As expected, the amount of reaction product decreases with the increasing gas flow. The photoactive materials that showed the fastest reaction rates were the ones that produced higher amounts of CO_2 and $COCl_2$. The data obtained with TiO_2-AcAc-F127 indicated that TCE photodegradation is high due to the formation of DCAC, explaining the lower CO_2 and $COCl_2$ amounts (see Section 3.2.2).

The influence of the complexing agent on the photocatalytic degradation of TCE is observed in Fig. 3. The TCE conversion along with TCE, CO_2 and $COCl_2$ concentration in the outlet are shown in this figure. The superior performance of the samples prepared with acetic acid is clearly observed, increasing the TCE conversion around 20%. Both materials have a similar refraction index (around 2.1) and similar contact angle. The different behaviour could be associated to the modification of the textural properties. Moreover, according to XRD results, acetic acid favours the formation larger TiO_2-anatase crystals and this feature seems to play an important role in the photocatalytic performance.

In order to optimize the effective use of photons by TiO_2, samples with different number of layers were prepared. The results obtained with samples synthesised with acetic acid and Brij 58, the ones that showed the best photocatalytic activity results, is shown in Fig. 4. A remarkable increase of the TCE conversion when the layer thickness changed from 160 to 240 nm, especially at a lower contact time, was observed. On the other hand, whereas the addition of a third layer increased the film thickness up to 360 nm it did not result in a significant change in the photocatalytic activity. Since thermal treatments at 350 °C/1 h were performed after the

deposition of each layer, the probable reduction of the porosity must be taken into account (Table 1) [48]. Consecutive heat-treatments likely collapsed the structure with the subsequent densification of the films. UV radiation penetrates only to a limited length and the diffusion of TCE molecules from the gas phase to the photocatalyst active sites is possibly inhibited by the increasing number of layers and the densification of the coating. Thus, the optimum thickness of the TiO_2 layer for maximum efficiency was set around 250 nm.

3.2.2. Effect of the relative humidity

Since vapour water goes along within polluted gas streams, the effect of the R.H. in the photocatalytic degradation of TCE was studied. Values of TCE degradation and reaction products concentration were taken at steady state conditions, in order to avoid the effect of irradiance and temperature during the heating of the lamps. Examples of the FTIR spectra taken at different relative humidity for TiO_2-AcOH-Brij 58 (250 nm) are shown in Fig. 5a. The ones corresponding to the 78% water vapour content are not shown for the sake of clarity. Trichloroethylene has a characteristic band centred at 960 cm^{-1}. In the absence of water vapour, the presence of CO_2 (2349 cm^{-1}), CO (2144 cm^{-1}), phosgene (1827 cm^{-1}) DCAC (1076 cm^{-1}) and HCl (2885 cm^{-1}) can be observed. The presence of water vapour in the feed leads to the appearance of two sets of strong bands between 4000–3400 cm^{-1} and 2100–1200 cm^{-1} overlapping with those of CO, $COCl_2$, DCAC and HCl. The signal corresponding to water was subtracted from the original spectrum (Fig. 5b). The intensity of the $COCl_2$ band is constant within 0–50% R.H. but decreased significantly at 78% R.H. Thus, a relationship between the CO_2/$COCl_2$ ratio and the water vapour content can be deduced.

TCE conversions as well as CO_2 and $COCl_2$ quantities at steady state conditions are shown in Fig. 6 for the different photocatalysts. The results corroborate the effects observed in the absence of water. Coatings prepared from sols with AcOH, dense or porous, record a higher photocatalytic activity than those deposited from
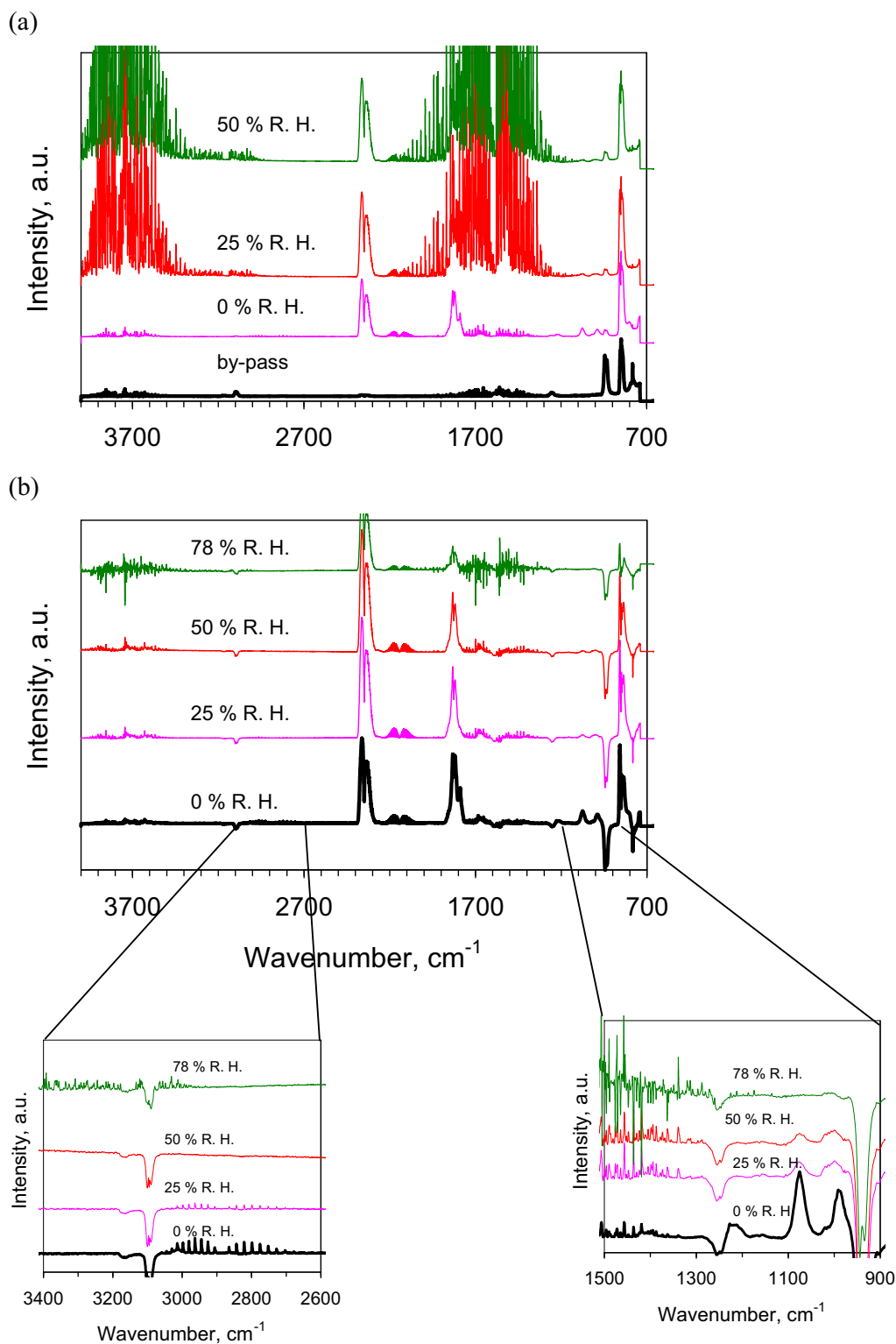
Fig. 5. (a) FTIR spectra collected at steady state conditions for TiO_2-AcOH-Brij 58 at different relative humidity content. (b) Subtraction spectra. Operating conditions: total flow: 200 ml min^{-1}, [TCE] = 90 ppm, R.H. = 0–80%.

sols with acetyl acetone. Moreover, the increase of the porosity due to the addition of surfactants improved the photocatalytic properties of the TiO_2 thin films even in the presence of high quantities of water vapour. The incorporation of water vapour at contents above 50% led to a drastic decrease of the photocatalytic activity and consequently to lower CO_2 and $COCl_2$ formation. This feature can be explained by considering that TCE and H_2O compete for

the same active sites. Fig. 7 shows the adsorption isotherm of the AcOH-Brij-58 coating obtained by spectral ellipsometry compared to the evolution of the TCE conversion. At low R.H., V_{ads}/V_{film} and TCE conversion changed very slowly. Above 50% R.H., V_{ads}/V_{film} sharply increased, associated to the filling of the pores with molecular water. As a consequence, the exposed surface decreased and therefore, TCE conversion began to fall. When the pores were prac-
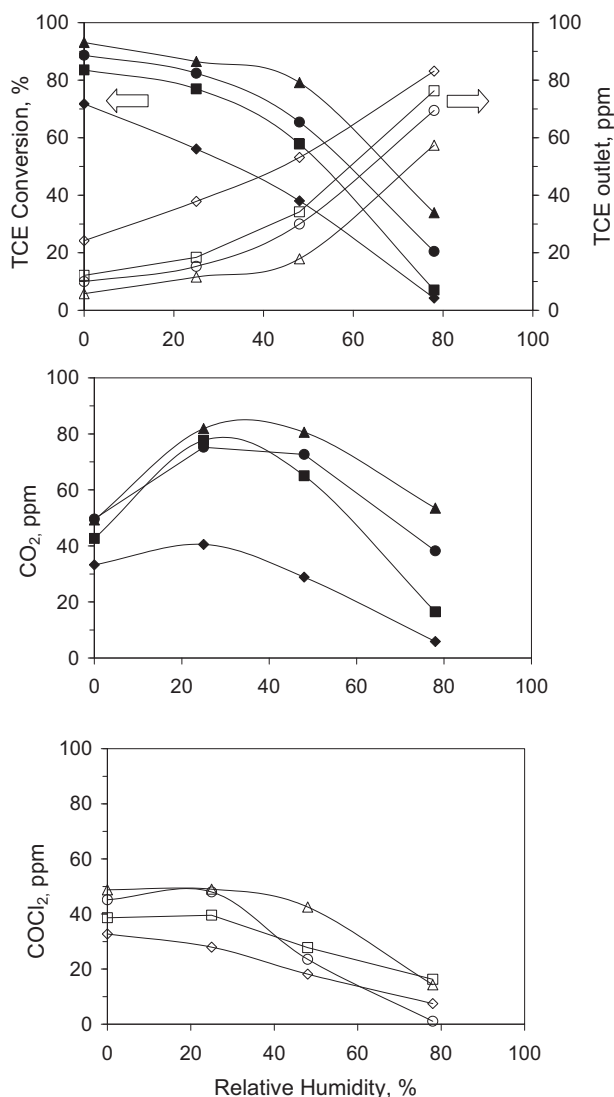
Fig. 6. Variation of the photocatalytic efficiency and main reaction products with the relative humidity for: TiO_2-AcOH-Brij58 (▲, △), TiO_2-AcAc-Brij 58 (■, □), TiO_2-AcOH (●, ○), TiO_2-AcAc (◆, ◇).
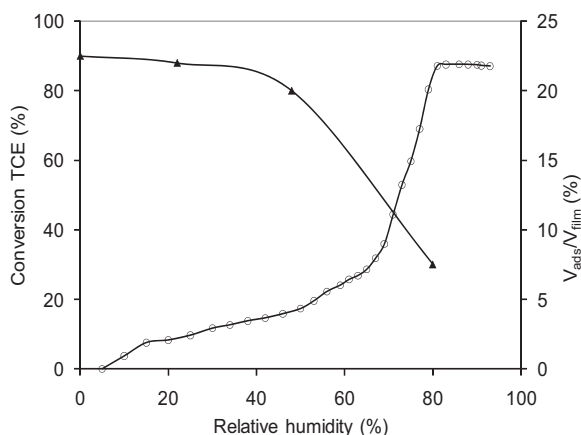
Fig. 7. Evolution of the V_{ads}/V_{film} (○) and TCE conversion (▲) with the relative humidity for TiO_2-AcOH-Brij58 sample.

tically full, condensation of water took place and TCE absorption was impeded because the surface suffered a violent decrease. This result is in line with the photocatalytic behaviour described above.

It is important to notice that TCE conversion was not modified within R.H. range between 0 and 50% but, on the contrary, mineralization was promoted. Considering that the amount of $COCl_2$ is constant in this R.H. range, the main reaction pathway at this condition is the direct decomposition of TCE into CO_2 according to Eq. (1).

$$C_2HCl_3 + \frac{3}{2}O_2 + H_2O \rightarrow 2CO_2 + 3HCl \tag{1}$$
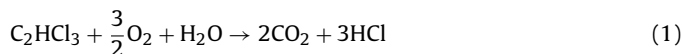
Nevertheless, others side reactions must be taken into consideration in order to justify the behaviour of $COCl_2$. One such possible reaction could be the direct oxidation of TCE (Eq. (2)) but at slower reaction rate than in the absence of water vapour in the stream.

$$C_2HCl_3 + \frac{3}{2}O_2 \rightarrow COCl_2 + HCl + CO_2 \tag{2}$$
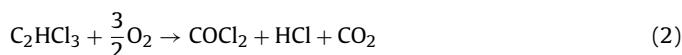
In the case of DCAC formation (data not shown) a progressive decrease of the reaction rate with water vapour content was observed. These results seem to indicate that the decomposition of DCAC into $COCl_2$ could be a side reaction pathway and a source of $COCl_2$ as previously suggested by Blake et al. [30,46] (Eqs. (3) and (4)). Thus, the net balance for $COCl_2$ was close to zero, and apparently no differences in the $COCl_2$ concentration were appreciated.

$$C_2HCl_3 + \frac{1}{2}O_2 \rightarrow C_2HCl_3O \tag{3}$$

$$C_2HCl_3O + \frac{1}{2}O_2 \rightarrow COCl_2 + HCl + CO \tag{4}$$
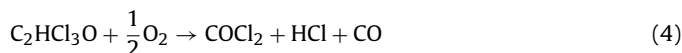
Our results show that the incorporation of hydroxyl groups from water vapour increases the TCE reaction rate for Eq. (1) but do not favour hydrolysis of $COCl_2$ at the operating conditions selected, as suggested by other authors [30–32].

Either (or both) increasing the residence time or including an adsorbent bed to promote the hydrolysis reaction [30] could be possible strategies to minimise the concentration of non desirable reaction compounds even in the presence of water vapour.

4. Conclusions

The incorporation of surfactants as pore generating agents resulted in titania coatings with smaller crystallite size, refractive index, and higher pore volume. The presence of mesoporosity reduces internal mass transfer limitations increasing the photocatalytic activity. The best results were obtained with TiO_2-AcOH-Brij58 coatings. The study on the influence of the complexing agent showed a better photocatalytic behaviour for the coatings prepared from the sol containing acetic acid with respect to those synthesised with acetyl acetone.

Finally, the effect of the R.H. in the photocatalytic degradation of TCE showed that the direct TCE oxidation pathway was favoured in the presence of water vapour. The quantification of the different reaction products have to be carefully analysed. Although a general overview of the FTIR spectra seems to indicate that the $COCl_2$ signal disappears, the subtraction of the water signal showed the formation of $COCl_2$. The concentration of $COCl_2$ did not change with water vapour content between 0 and 50% R.H., suggesting that the hydrolysis reaction did not take place under the reaction conditions studied here.

Appendix A.   Supplementary data

Supplementary data associated with this article can be found, in the online version, at doi:10.1016/j.apcatb.2011.07.027.

References

[1] M.A. Fox, M. Dulay, Chem. Rev. 93 (1993) 341.
[2] T.T. Shen, C.E. Schmidt, T.R. Card, Assessment and Control of VOC Emissions from Waste Treatment and Disposal Facilities, Van Nostrand Reinhold, New York, 1993.
[3] A.L. Hines, T.K. Ghosh, S.K. Loyalka, R.C. Warder Jr., Indoor Air, Quality and Control, PTR Prentice Hall, Englewood Cliffs, NJ, 1993, ISBN 0-13-463977-4, p. 340.
[4] O. Carp, C.L. Huisman, A. Reller, Prog. Solid State Chem. 32 (2004) 33.
[5] S. Suarez, J.M. Coronado, R. Portela, J.C. Martín, M. Yates, P. Avila, B. Sanchez, Environ. Sci. Eng. 42 (2008) 5892.
[6] T.L.R. Hewer, S. Suárez, J.M. Coronado, R. Portela, P. Avila, B. Sanchez, Catal. Today 13 (2009) 302.
[7] X. Chen, S.S. Mao, Chem. Rev. 107 (2007) 2891.
[8] E. Scolan, C. Sanchez, Chem. Mater. 10 (1998) 3217.
[9] M. Wu, G. Lin, D. Chen, G. Wang, D. He, S. Feng, R. Xu, Chem. Mater. 14 (2002) 1974.
[10] M.J. Percy, J.R. Bartlett, J.L. Woolfrey, L. Spiccia, B.O. Westa, J. Mater. Chem. 9 (1999) 499.
[11] J.A. Chang, M. Vithal, I.C. Baek, S.I. Seok, J. Solid State Chem. 182 (2009) 749.
[12] U. Schubert, J. Mater. Chem. 15 (2005) 3701.
[13] T. Kitamura, H. Kumazawa, Chem. Eng. Commun. 192 (2005) 795.
[14] Y. Kotani, T. Matoda, A. Matsuda, T. Kogure, M. Tatsumisago, T. Minami, J. Mater. Chem. 11 (2001) 2045.
[15] N. Nobuaki, T. Koji, I. Takashi, J. Sol-Gel Sci. Technol. 13 (1998) 691.
[16] J.G. Yu, X.J. Zhao, Q.N. Zhao, Thin Solid Films 379 (2000) 7.
[17] Y. Chen, S. Lunsford, D.D. Dionysiou, Thin Solid Films 516 (2008) 7930.
[18] A.A.C. Magalhães, D.L. Nunes, P.A. Robles-Dutenhefner, E.M.B. de Sousa, J. Non-Cryst. Solids 348 (2004) 185.
[19] E. Stathatos, P. Lianos, C. Tsakiroglou, Micropor. Mesopor. Mater. 75 (2004) 255.
[20] H. Choi, E. Stathatos, D.D. Dionysiou, Appl. Catal. B 63 (2006) 60.
[21] Y. Chen, E. Stathatos, D.D. Dionysiou, Surf. Coat. Technol. 202 (2008) 1944.
[22] A. Testino, I.R. Bellobono, V. Buscaglia, C. Canevali, M. D'Arienzo, S. Polizzi, R. Scotti, F. Morazzoni, J. Am. Chem. Soc. 129 (2007) 3564.
[23] H. Cheng, J. Ma, Z. Zhao, L. Qi, Chem. Mater. 7 (1995) 663.
[24] (a) R.R. Bacsa, J. Kiwi, Appl. Catal. B 16 (1998) 19;
    (b) D. Gumy, C. Morais, P. Bowen, C. Pulgarin, S. Giraldo, R. Hajdu, J. Kiwi, Appl. Catal. B 63 (2006) 76.
[25] T. Peng, D. Zhao, K. Dai, W. Shi, K.J. Hirao, Phys. Chem. B 109 (2005) 4947.
[26] H. Yin, Y. Wada, T. Kitamura, S. Kambe, S. Murasawa, H. Mori, T. Sakata, S. Yanagida, J. Mater. Chem. 11 (2001) 1694.
[27] N. Arconada, A. Durán, S. Suárez, R. Portela, J.M. Coronado, B. Sanchez, Y. Castro, Appl. Catal. B 86 (2009) 1.
[28] W.A. Zeltner, C.G. Hill, M.A. Anderson, Chem. Tech. 127 (3) (1993) 21.
[29] S. Yamazaki-Nishida, K. Pagano, L.A. Phillips, S. Cervera-March, M.A. Anderson, J. Photochem. Photobiol. A 70 (1) (1993) 95.
[30] W.A. Jacoby, M.R. Nimios, D.M. Blake, Environ, Sci. Technol. 28 (1994) 1661.
[31] J. Fan, J.T. Yates, J. Am. Chem. Soc. 118 (1996) 4686.
[32] P.B. Amama, K. Itoh, M. Murabayashi, J. Mol. Catal. A 176 (2001) 165.
[33] N. Arconada, Y. Castro, A. Durán, Appl. Catal. A: Gen. 385 (2010) 101.
[34] J. Yu, X. Zhao, Mater. Res. Bull. 35 (2000) 1293.
[35] C. Boissiere, D. Grosso, S. Lepotre, L. Nicole, A. Brunet Bruneau, C. Sánchez, Langmuir 21 (2005) 12362.
[36] G. Atanassov, R. Thielsch, D. Popov, Thin Solid Films 233 (1993) 288.
[37] H. Choi, Novel preparation of nanostructured titanium dioxide photocatalytic particles, films, membranes and devices for environmental applications, Thesis, University of Cincinnati, 2007.
[38] M.S. Lee, S.S. Park, G.-D. Lee, C.-S. Ju, S.-S. Hong, Catal. Today 10 (2005) 283–290.
[39] P.C. Angelomé, M.C. Fuertes, J.A.A. Soler-Illia, Adv. Mater. 18 (2006) 2397–2402.
[40] Y. Djaoued, S. Badilescu, P.V. Ashrit, D. Bersani, P.P. Lottici, J. Sol-Gel Sci. Technol. 520 (24) (2002) 247.
[41] S. Inagaki, Y. Fukushima, Micropor. Mesopor. Mater. 21 (1998) 667.
[42] C. Ookaa, H. Yoshida, M. Horio, K. Suzuki, T. Hattori, Appl. Catal. B 41 (2003) 313.
[43] A. Borrás, A. Yanguas-Gil, A. Barranco, J. Cotrino, A.R. González-Elipe, Phys. Rev. B 76 (2007) 235303.
[44] P.I. Ravikovitch, A.V. Neimark, Lagmuir 18 (2002) 1550.
[45] S. Hata, Y. Kai, I. Yamanaka, H. Oosaki, K. Hiroto, S. Yamagishi, JSAE Rev. 21 (2000) 97.
[46] M.R. Nimios, W.A. Jacoby, D.M. Blake, T.A. Milne, Environ. Sci. Technol. 27 (1993) 732.
[47] M.D. Driessen, A.L. Goodman, T.M. Millar, G.A. Zaharias, V.H. Grassian, J. Phys. Chem. B 102 (1998) 549.
[48] D.W. Bahneman, S.N. Khluiskaya, R. Dillert, A.I. Kulak, A.I. Kokorin, Appl. Catal. B 36 (2002) 161.